Published in final edited form as:
Mol Cancer Ther. 2011 December ; 10(12): 2287–2297. doi:10.1158/1535-7163.MCT-11-0536.

Micelle-encapsulated thiostrepton as an effective nanomedicine for inhibiting tumor growth and for suppressing FOXM1 in human xenografts

Ming Wang[1] and **Andrei L. Gartel**[1,2,3,*]

[1]Department of Medicine, University of Illinois at Chicago, Chicago, IL, 60612, USA

[2]Department of Biochemistry and Molecular Genetics, University of Illinois at Chicago, Chicago, IL, 60607, USA

[3]Department of Microbiology and Immunology, University of Illinois at Chicago, Chicago, IL, 60612, USA

Abstract

The thiazole antiobiotic, thiostrepton, has been found to induce cell death in cancer cells through proteasome inhibition. As a proteasome inhibitor, thiostrepton has also been shown to suppress the expression of FOXM1, the oncogenic forkhead transcription factor overexpressed in cancer cells. In this study, we explored the potential *in vivo* anticancer properties of thiostrepton, delivered through nanoparticle encapsulation to xenograft models of breast and liver cancer. We encapsulated thiostrepton into micelles assembled from amphiphilic lipid-PEG (polyethylene glycol) molecules, where thiostrepton is solubilized within the inner lipid compartment of the micelle. Upon assembly, hydrophobic thiostrepton molecules are solubilized into the lipid component of the micelle shell, formed through the self assembly of amphipilic lipid-PEG molecules. Maximum accumulation of micelle-thiostrepton nanoparticles (100nm in diameter, −16mV in zetapotential) into tumors was found at 4 hours post-administration and was retained for at least 24 hours. Upon continuous treatment, we found that nanoparticle-encapsulated thiostrepton reduced tumor growth rates of MDA-MB-231 and HepG2 cancer xenografts. Furthermore, we show for the first time the *in vivo* suppression of the oncogenic FOXM1 after treatment with proteasome inhibitors. Immunoblotting and immunohistochemical staining also showed increased apoptosis in the treated tumors, as indicated by cleaved caspase-3 expression. Our data suggest that the thiazole antibiotic/proteasome inhibitor thiostrepton, when formulated into nanoparticles, may be highly suited as a nanomedicine for treating human cancer.

Keywords

apoptosis; cancer; FOXM1; micelles; nanomedicine

Introduction

As the second most common cause of mortality in the US, cancer poses as a disease that requires urgent improvement of therapeutic strategies. Originally adopted for the topical treatment of veterinary dermatological infections, thiostrepton, a thiazole antibiotic, has also been shown to inhibit cell growth in a variety of human cancer cell lines (1–3). The

*Correspondence: Andrei L. Gartel, University of Illinois at Chicago, Department of Medicine, 840, S. Wood St., Room 1041, Chicago, IL 60612, (312) 996-1855 (Telephone), (312) 996-8697 (Fax), agartel@uic.edu.

apoptotic activity of thiostrepton has been deciphered to be through proteasome inhibition (3–5), resulting in the stabilization of certain proteins which proves fatal to cancer cells. However, one target observed to be suppressed rather than stabilized is that of the forkhead box M1 transcription factor, FOXM1 (3, 6), a protein found to be over-expressed in a variety of human cancers (7–9). It has been suggested that the inhibition of FOXM1 by proteasome inhibitors may contribute to their anticancer activity (6).

Upon discovery, major issues associated with current anti-cancer drugs such as paclitaxel and tamoxifen were their insolubilities in aqueous solutions (10, 11). Methods to overcome such obstacles included the encapsulation of the drugs into amphiphilic nanoparticle systems, amphiphilic in that they possess a hydrophilic outer shell and a hydrophobic inner core in which the hydrophobic drugs can be solubilized (12–14). Encapsulation into nanoparticles acts not only as a means to solubilize hydrophobic drugs, but as importantly, the association of cancer drugs into nanomeric structures aids their specific accumulation into tumor sites. Compared to those of healthy, non-cancerous tissues, the neovasculature that supplies blood flow to tumors is highly irregular and punctuated with fenestrations. These junctions provide openings with sizes of 700nm across, increasing their permeability to particles smaller than 700nm in diameter (15). Unlike small molecules, nano-sized macromolecules are less toxic to healthy organs and non-cancerous tissues, as they leave circulation only *via* diffusion through the fenestrated gaps of tumor blood vessels (16–18). The clinical application of proteasome inhibitors as chemotherapeutic agents has also been associated with levels of high toxicity, and is likely to benefit from nanoparticle-protected delivery (19–21).

Like the case of other hydrophobic cancer drugs, the first limitation in showcasing thiostrepton as a chemotherapeutic solution is its insolubility in aqueous solutions. As a lucid and simple method, the use of PEGylated lipids has been described as a means to solubilize hydrophobic drugs into macromolecular delivery vehicles (12, 22, 23). As the encapsulation of proteasome inhibitors into nanoparticulate delivery systems for cancer treatment has yet to be described, we carried out this study in order to investigate the possibility of inducing an enhanced anti-tumor effect using micelle-encapsulated thiostrepton.

Materials and Methods

Cell lines and chemical compounds

MDA-MB-231-luc-D3H2-LN, human lymph node-derived metastatic mammary gland adenocarcinoma (Caliper Lifescience); HepG2-luc, human hepatocellular carcinoma stably transfected with luciferase-expressing gene (retrovirus). MDA-MB-231 cells were maintained in MEM media (Mediatech) supplemented with 10% FBS (Atlanta Biological), 1% 100X non-essential amino acids (Gibco), 1% 200mM NaPyruvate (Gibco) and 75μg/mL Zeocin (Invitrogen). HepG2-luc cells (ATCC) were kept in DMEM media supplemented with 10% FBS and 1% Penicillin/streptomycin (Gibco). Cells had not been authenticated by authors. 1,2-distearoyl-sn-glycero-3-phosphoethanolamine-N-[methoxy(polyethylene glycol)-2000] (DSPE-PEG_{2000}-MeO) and 1,2-dioleoyl-sn-glycero-3-phosphoethanolamine-N-(lissamine rhodamine B sulfonyl) (Rhodamine-DOPE) was purchased from Avanti Polar Lipids. Thiostrepton (from Streptomyces azureus, 90% purity) was obtained from Sigma.

Preparation of polymeric micelle-encapsulated thiostrepton

A thin lipid-film of DSPE-PEG_{2000}-MeO and thiostrepton was prepared by mixing the two components in chloroform in a 10mL round-bottomed flask. The chloroform was removed *in vacuo* and by air-drying, after which the lipid film was hydrated (for final thiostrepton

concentration of 1mM or 2mM) with PBS (pH7) or H_2O and vortexed at room temperature for 10mins. The lipid-to-drug ratio was varied by keeping the amount of thiostrepton constant (at 1mM) and increasing the amount of PEG-lipid from 1 to 4mM. The percentage of encapsulated thiostrepton was measured by centrifuging solutions of micelle-thiostrepton (varying lipid-to-drug ratios) at 8RCF for 2mins, after which the supernatant was separated from any precipitated matter (insoluble, unencapsulated thiostrepton). The supernatent was measured for UV absorbance at λ=300nm, from which the amount of remaining encapsulated thiostrepton was calculated. To measure the amount of non-encapsulated thiostrepton, the precipitates were dissolved in $CHCl_3$ and examined for UV absorbance at λ=300nm. For micelle-only preparations, the thiostrepton component was omitted and only the lipid component was hydrated in aqueous solution to 3mM or 6mM, corresponding to either 1mM thiostrepton or 2mM thiostrepton. For fluorescence labeling, DOPE-Rhodamine was incorporated at the chloroform stage at a 1:100 molar ratio to DSPE-PEG_{2000}-MeO.

Physical characterization of micelle-encapsulated thiostrepton

For drug release studies, micelle-thiostrepton suspensions (3:1 or 4:1 lipid/drug ratios m/m) were incubated in 50% FBS (in PBS, final concentrations of 0.05mM thiostrepton) over time at 37°C. Amount of remaining encapsulated thiostrepton was measured by centrifuging incubated samples (8RCF, 2mins) to remove the non-encapsulated and precipitated thiostrepton from the micelle-encapsulated thiostrepton in the supernatent. The supernatant was then measured for UV absorbance at λ=300nm and the concentration of remaining thiostrepton was calculated by extrapolation with calibration curves. Sizes and zetapotentials of nanoparticles (in PBS) were analyzed by dynamic light scattering, using a 5mW 633nm laser angled at 90° to the sample. Measurements are presented as volume-weighted multimodal distributions. For *in vitro* and *in vivo* applications, micelle-encapsulated thiostrepton solutions were prepared in PBS (sterile) at 1mM or 2mM, respectively. For transmission electron microscopy, 20μL of micelle-thiostrepton solutions (1mM thiostrepton/3mM lipid) or micelle-only solutions (3mM lipid) in H_2O were dispensed onto a 200-mesh Cu grid supported by holey-carbon film and air-dried overnight. TEM images were collected using the JEOL JEM-3010, equipped with a LaB6 electron gun operated at 300kV. Images were captured using a 1K × 1K Peltier-cooled Gatan multi-scan CCD camera.

Treatment of cells in vitro

MDA-MB-231 cells were seeded at 1×10^5 cells/10cm plate and HepG2-luc cells were seeded at 5×10^5 cells/6cm plate and incubated overnight before treatment. Non-encapsulated thiostrepton (dissolved in DMSO, 10mM) and micelle-encapsulated thiostrepton (1mM) were administered to cells at concentrations of 5 μM, 7.5 μM and 10μM. Controls for *in vitro* experiments were cells treated with either DMSO only (6μL) or micelle-only (30μM). Cells were treated for 24 hours before harvesting.

Western Blot analysis of cell lysates

Cells were harvested with IP lysis buffer (20mM HEPES, 1% Triton X-100, 150mM NaCl, 1mM EDTA, 1mM EGTA, 100mM NaF, 10mM $Na_4P_2O_7$, 1mM Na_3VO_4, 0.2mM PMSF). For analysis of tissues, liquid N_2-frozen sections of xenograft tumors were homogenized in 1mL IP lysis buffer. Protein concentration was measured by the Bio-Rad Protein Assay and protein separation was performed on 8% or 12% SDS-PAGE gels. Separated proteins were then transferred onto PVDF membranes (Millipore) and immunoblotted with specific antibodies against FOXM1 (c-20, Santa Cruz), cleaved-caspase-3 (Cell signaling) and β-actin (Sigma) (24). Quantification of cleaved caspase-3 and FOXM1 protein expression levels was performed by the 'Gel' analysis function in ImageJ.

Cell viability assay

Cells were seeded at a density of 1000 cells/well into 96 well plates. After incubation overnight, growth media was replaced with media containing free (in DMSO) or micelle-encapsulated thiostrepton at increasing concentrations. DMSO-treated and micelle-only-treated cells were also examined and used to compare with non-treated (media only) cells. Cells were treated for 72 hours before media was spiked with 3-(4,5-dimethylthia-zol,2-yl)-2,5-diphenyltetrazolium bromide (MTT) assay reagent (Sigma, prepared in 5mg/mL in PBS) to render a final 10% concentration. After incubation for 3 hours, MTT/media was removed and purple precipitates were dissolved with 150μL of DMSO. Wells were measured for absorbance at λ= 550nm and the % cell viability was calculated as a percentage of the UV absorbance of non-treated cells.

Animal maintenance and tumor xenograft experiments

Animals were maintained and treated in accordance with the guidelines established by the Animal Care and Use Committee of UIC. Tumor models were prepared by implanting cancer cell lines (1×10^6 of MDA-MB-231 and 2×10^6 of HepG2-luc), suspended in 50uL of 1:1 PBS/Matrigel into each flank of 4-week old male athymic mice (Taconic). Treatment began once tumors reached sizes of $30mm^3$ or $150mm^3$. After completion of the dosing schedule, animals were sacrificed and tumors were removed. Tumors were sliced in half and either frozen in liquid N_2 or fixed overnight in 10% formalin (4°C).

Biodistribution of micelle-thiostrepton nanoparticles

Rho-labeled micelle-thiostrepton nanoparticles were injected *via* the tail-vein into non-tumor-bearing or MDA-MB-231 tumor-bearing animals ($1cm^3$ per tumor) at a dose of 1.8mg thiostrepton per animal. At 4hrs, 17hrs and 24hrs post-injection, animals were anaesthetized with isoflurane and imaged using the Xenogen IVIS system for rhodamine-fluorescence distribution. Animals were then sacrificed and organs removed for further fluorescence imaging. Background autofluorescence was eliminated using a spectral unmixing algorithm provided by Living Image software. For comparison with free, non-micelle-encapsulated drug, thiostrepton was dissolved to concentrations of 36mg/mL in a *N*,*N*-dimethylacetamide/polyethylene glycol/Tween 80 formulation (2:7:1) (25) and administered at a dose of 50μL per animal (2 animals, total 4 tumors) by *i.p.* injection. Tumors were collected at 4 hours and 24 hours post-injection and were homogenized (Fisher, Polytron) in 1mL lysis buffer. Tumor homogenates were treated with 200μL 10mM HCl for 24 hours at 4°C. 1mL of chloroform was then added and the homogenates were vortexed for 10 mins. Samples were incubated at room temperature for 24 hours before vortexing, after which samples were centrifuged and the chloroform supernatent layer was collected and dried *in vacuo*. For HPLC/Mass spectrometry studies, extracted samples were reconstituted in 50μL of chloroform and 450μL of MeOH. Using an Agilent Zorbax 300sb-C8, 2.1×50mm column, the isocratic method of 30% of 100% H_2O/0.1% Formic acid and 70% of 100% Methanol/0.1% Formic acid at 200μl/ml for 6 Minutes was run. The AUC of HPLC traces that correlated to thiostrepton retention times were used to calculate the concentrations of thiostrepton, as compared to a thiostrepton/HPLC calibration curve.

Treatment of xenograft models with micelle-encapsulated thiostrepton

Animals bearing tumors were randomized into groups of 4–5, where groups were administered with micelle-only controls at 200mg DSPE-PEG_{2000}-MeO/kg, (200–250uL of 6mM DSPE-PEG_{2000}-MeO in PBS) or 30–40mg/kg of thiostrepton encapsulated in micelles (2mM thiostrepton/6mM DSPE-PEG_{2000}-MeO in PBS, 200–300uL). Treatments were performed once every two days (3 times a week), during which tumor volumes were monitored with calipers ($l \times w \times h$ = volume, mm^3). In the MDA-MB-231 model, injections

were carried out daily for the last 5 days. Animals were also weighed once a week. After 12–14 treatments, animals were sacrificed and tumors removed.

Immunohistochemical analysis of paraffin-embedded tissue

Formalin-fixed tumor tissues were embedded in paraffin and sliced to 4μm-thick sections. Sections were deparaffinzed by submerging sample-containing slides into a series of solvents of decreasing hydrophobicity. Heating samples in 10mM citric acid (pH 6) was used for antigen retrieval. After blocking with 3% H_2O_2 in MeOH, and further blocking in normal goat serum in PBS, slides were treated with primary anti-FOXM1 (Santa Cruz, k-19), anti-cleaved caspase-3 or control IgG antibodies at concentrations of 1:100, in 1% BSA/PBS. Biotinylated secondary antibody treatment and Avidin HPR treatment was carried out according to the Vectastain ABC kit manual (anti-rabbit, Vector Labs), followed by staining with DAB (Sigma, D-0426). Cleaved caspase-3-stained samples were counterstained with hematoxylin (Vector Labs). Samples were dehydrated in the series of solvents and mounted with Permount (Fisher) mounting agent. Slides were analyzed on a Zeiss Apotome microscope.

Results

Preparation of micelle-encapsulated thiostrepton

The purpose of this study was to formulate thiostrepton, a highly hydrophobic anticancer drug into nanoparticle delivery vehicles and to examine its effect as a nanomedicine against cancer *in vivo.* Encapsulation of thiostrepton (Figure 1, a) into nanomeric micelles was conducted by using the lipid-hydration method, and encapsulation conditions were optimized by varying the lipid-to-thiostrepton ratio. The lipid considered for this application was DSPE-PEG_{2000}-MeO (Figure 1, a), a polymer-lipid conjugate chosen for its ability to spontaneously form micelles with hydrophobic cores upon dispersion in aqueous solutions (22). PEGylated lipids are amphiphilic lipid-polymer conjugates where the polymer component is a hydrophilic polymer chain such as polyethylene glycol (PEG). Upon hydration, these lipid-PEG conjugates form amphiphilic micellar structures consisting of a hydrophilic polymer shell, and an organic lipidic core (Figure 1, b). It is within this lipid-rich area that thiostrepton can be solubilized and ultimately incorporated into nano-sized macromolecular structures which can aid its accumulation into tumor sites (26–28). At concentrations above reported critical micelle concentrations (23, 29), various drug-to-lipid ratios were examined for their drug encapsulation efficiency (Figure 1, c). By keeping the concentration of thiostrepton constant at 1mM and increasing the concentration of DSPE-PEG_{2000}-MeO, it was found that highest encapsulation efficiencies were obtained after lipids outnumbered thiostrepton molecules by 3 fold (3:1 PEG-lipid/thiostrepton, m/m), after which there was no significant increase in amount of thiostrepton encapsulated. The optimal formulation of 3:1 DSPE-PEG_{2000}-MeO/thiostrepton (m/m) was chosen to be used for studying the effect of nanoparticle-encapsulated thiostrepton on cancer cells. Assembled micelle-thiostrepton structures were found to be in the form of nanoparticular structures with hydrodynamic dimensions of 100nm in diameter and −16mV in zetapotential (Figure 2, a).

An inherent negative charge (negative zetapotential) on the surfaces of nanoparticles is desirable for delivery to tumor sites, as to prevent opsonin recognition which could lead to macrophage-assisted clearance from circulation (30, 31). Opsonization, the immune response action of tagging positively charged alien particles with negatively charged opsonin proteins should be minimized as to avoid clearance by macrophage recognition (32). Transmission electron microscopy images illustrated the difference in micelles before and after drug encapsulation and confirm the presence of 100nm-diameter micelle-thiostrepton species (Figure 2, b). The release profile of the optimal formulation were

examined by incubating micelle-thiostrepton nanoparticles (3:1 lipid/drug, m/m) in PBS solutions containing 50% FBS at 37°C, to mimic the plasma serum conditions of *in vivo* blood circulation (Figure 2, c). In 50% FBS, the integrity of the micelle-thiostrepton structure was maintained for long periods of time, where 90% of thiostrepton was retained within nanoparticle structures after 24 hours of incubation. This finding is particularly significant for the *in vivo* application of such nanoparticles, where the maintenance of drug encapsulation in circulation for longer periods is required for accumulation into tumor sites.

Micelle encapsulation enhances apoptotic effect of thiostrepton on breast cancer and liver cancer cells in vitro

Treatment of MDA-MB-231 breast cancer and HepG2-luc (luciferase-expressing) liver cancer cells with micelle-encapsulated thiostrepton resulted in an enhancement of cleaved caspase-3 expression (a marker of apoptosis), compared to those treated with non-encapsulated thiostrepton (Figure 3, a, b). Also observed is the further suppression of FOXM1, in cells treated with micelle-encapsulated thiostrepton, compared to free thiostrepton. As thiostrepton is highly insoluble (precipitates of DMSO-dissolved thiostrepton are highly visible when added to cell media), it is likely that its full encapsulation into micelles increases its availability to cancer cells *in vitro*. Cell viability assays also confirmed the enhanced effect of thiostrepton, when delivered to cells through micelle-encapsulation (Figure 3, c, d). In terms of mechanism of drug internalization within the cancer cells, it is likely that thiostrepton is released into the cell media before it is internalized into cancer cells, as incubation with fluorescently-labeled micelle-thiostrepton did not show cell-associated fluorescence over time (Supplementary data, S1). As for empty micelles, they alone did not have an effect on cell viability, suggesting their low toxicity for *in vivo* applications.

Accumulation of micelle-encapsulated thiostrepton into MDA-MB-231 breast cancer xenografts and its effect on tumor growth

Nano-sized particles can localize specifically into tumor sites by bypassing healthy tissue and diffusing through the leaky fenestrations in the tumor blood vessels, a vascular characteristic shared with no other organ apart from the liver (33). Further to their specific localization, nano-sized structures are retained in tumor sites due to the impaired lymphatic drainage system of tumor tissue (16). The ability of administered micelle-thiostrepton to localize into tumors was investigated using nude mice bearing MBA-MB-231 xenografts. The tumor retention and biodistribution of micelle-thiostrepton was studied by LC/MS of the tumor homogenates and by live animal fluorescence imaging.

Upon establishment of subcutaneous tumors, fluorescently-labeled micelle-thiostrepton was administered through the tail vein and animals were monitored for rhodamine-associated fluorescence by live whole body imaging (Xenogen IVIS). Accumulation of fluorescence into tumor sites (live and *ex vivo* imaging) was observed to occur to a maximum at 4 hours post-administration (Figure 4, a). Localization into the liver was also prominent at 4 hrs post-administration, likely an event of diffusion through the sinusoidal capillaries (33, 34), which are also punctuated with fenestrations as it is in angiogenic tumor vessels. By 17 hours, micelle-associated fluorescence had greatly diminished in tumor regions, although a small amount appeared retained. As fluorescence labeling only monitors the movement and retention of the lipid moiety of the micelle-thiostrepton complex, tumor homogenates were further extracted with chloroform (in which thiostrepton is soluble) and the amount of tumor-accumulated thiostrepton was examined using LC/MS. It was found that tumor-associated thiostrepton was in fact in higher concentrations at 24 hours post-injection, compared to that at 4 hours post-injection (Figure 4, b). In conjunction with the fluorescence-biodistribution data, this is indicating that micelle-thiostrepton complexes

arrive at tumor sites intact, and that it is also likely that thiostrepton continues to accumulate into tumors 4 hours post-administration (up until 17 hours), after which dissociation of the micelle-thiostrepton occurs and the lipid component is cleared from the region. Furthermore, the percentage ID (injected dose) of micelle-thiostrepton to arrive at tumors was approximately 30% per tumor, and considering there were two xenograft tumors per animal, 60% of the ID was tumor-localized (Figure 4, b). We compared the tumor accumulation of micelle-thiostrepton with that of its solubilization into the previously reported *N*,*N*-dimethylacetamide/polyethylene glycol/Tween 80 formulation (25) and found that micelle-encapsulated thiostrepton accumulated into tumors with greater efficiency, where an increase in approximately 10-fold of thiostrepton concentrations were detected in each tumor (Figure 4, b). In addition, pilot studies also showed the effect on xenograft growth of thiostrepton delivered through the dimethylacetamine-based formulation was much weaker in MDA-MB-231 tumors compared to delivery through micelle-encapsulation (data not shown).

The biological effect of micelle-encapsulated thiostrepton on tumor growth was monitored in MDA-MB-231 subcutaneous tumor models. The specific dose for administration (40mg/kg) was selected after pilot studies showed it to be the minimal concentration to exhibit anti-cancer effects. Injections were administered 3 times a week, which after 14 treatments, reduced tumor growth by up to 4-fold, compared to non-treated tumors (Figure 4, c). As determined from the release studies, it is likely that thiostrepton is not released from the micellar vehicle before it reaches the tumor sites, as thiostrepton can remain encapsulated for at least 24 hours in high serum conditions. Internalization of whole rhodamine-labeled micelle-thiostrepton complexes were shown to be possible at higher serum conditions, as indicated by increase in cell associated fluorescence over time (Supplementary data, S1). Therefore, it is likely that micelle-thiostrepton complexes arrive intact at tumor vicinities and are internalized into the tumor cells by mechanisms such as endocytosis. As with non-treated tumors, tumors treated with an equivalent dose of empty micelles (without thiostrepton) increased steadily in size over time, and a reduction in tumor growth rate was not observed (Figure 4, c). Final tumor weights of harvested tumors also correlated to tumor volume data, where non-treated tumors were on average 4 times heavier than micelle-thiostrepton-treated tumors (Figure, 4, d, e).

Micelle-encapsulated thiostrepton inhibits tumor growth in a HepG2-luc liver cancer subcutaneous xenograft model

Subcutaneous HepG2-luc liver cancer cells were left to proliferate until the size of the liver cancer xenografts reached 200mm^3, as to examine the effect of thiostrepton treatment on already larger tumors. As in the previous tumor model, the accumulation of micelle-thiostrepton into HepG2-luc xenografts was proven using rhodamine-associated whole body imaging (Supplementary data, S2). Doses were then administered at 30mg/kg, 3 times a week for 4 weeks and tumor progression was monitored by both caliper measurements and luciferase imaging. Again, the specific dose was chosen after pilot studies suggested it to be the minimum at which an effect can be observed in this model tumor. After completion of the dosing schedule, micelle-thiostrepton-treated tumors were found to be half the volume of the non-treated groups (Figure 5, a). The implanted HepG2-luc tumors also express luciferase proteins, therefore, their change in luciferase expression during the dosing gave insight into tumor cell viability. Compared to that of Day 0 (day of beginning of treatment), tumor-associated luciferase in micelle-thiostrepton-treated tumors was much less than that of non-treated tumors (Supplementary data, S3). After the treatment schedule, tumors were also removed and weighed, and treated tumors were found to be half the weight of non-treated tumors (Figure 5, b, c).

Removed tumors from xenograft models were then analyzed for markers of apoptosis by western blot and immunohistochemistry. Homogenized tumors showed overall an evident increase in the expression of cleaved-caspase-3, a marker of apoptosis (Figure 6, a). Furthermore, for the first time, it is shown that the treatment of *in vivo* cancers with thiostrepton, or any proteasome inhibitor leads to suppression of the cancer-associated transcription factor, FOXM1. Immunohistochemistry of tumor samples reinforce the effect found in homogenized tumors, where the expression of cleaved-caspase-3 is higher and FOXM1 levels are lower in micelle-treated tumors, compared to non-treated tumors (Figure 6, b).

Discussion

In this report, we aimed to highlight two main findings related to thiostrepton-based cancer therapy. Firstly, we showed that the encapsulation of thiostrepton into nanomeric micelles greatly enhances its solubility and particularly optimizes its tumor-associated biodistributional profile upon *in vivo* administration. Secondly, we demonstrated that the treatment of xenograft tumors with nanoparticle-thiostrepton results in reduced tumor growth rate, accompanied by molecular changes such as the suppression of the FOXM1 protein and induction of cell death indicated by caspase-3 cleavage.

Thiostrepton, the FOXM1/proteasome inhibitor is highly insoluble, therefore we employed a non-covalent solubilization method, using the polymer-lipid conjugate DSPE-PEG_{2000}-MeO to encapsulate thiostrepton within its lipophilic compartment (12, 23, 27, 35). The essential feature of using the DSPE-PEG_{2000}-MeO PEG-lipid conjugate to solubilize hydrophobic drugs lies of in the conjugate's ability to spontaneously self-assemble into nanomeric structures upon suspension in aqueous solutions (36, 37). Particles of nanometer dimensions have abilities to selectively target tumors, as opposed to the non-selectivity of non-encapsulated small molecule drugs. Once in circulation, nanoparticles bypass healthy tissue and organs to localize specifically in cancers (and the liver) due to their diffusion through the fenestrations within tumor-associated vasculatures. Blood vessels supplying non-cancerous tissues are usually highly regular, whereas those of tumors are irregular and leaky, a result of rapid angiogenesis evolved for tumor growth.

Our final micelle-thiostrepton nanoparticles were found to be around 100nm in diameter and −16mV in zetapotential. These two characteristics are advantageous for cancer-specific delivery, as illustrated by the biodistributional and tumor-accumulation data in breast and liver cancer xenograft models (Figure 4, a, b and S2). Small diameters are required for diffusion through tumor vasculature, and negative surface charges can prolong the circulation times of nanoparticles by preventing their adsorption of Kupffer cell-recognizable protein tags, hence enhancing their accumulation into tumor sites (36, 38). The tumor specificity of nanoparticles also increases the concentration of tumor-localized thiostrepton, where a 6-fold increase in thiostrepton was detected in tumors treated with micelle-encapsulated thiostrepton, compared to those treated with non-micelle-encapsulated thiostrepton (Figure 4, b). Prolonged retention of nanoparticulate structures in tumors, compared to livers, is likely due to the lack of lymphatic drainage associated with tumors (39–41). It appears that accumulation of nanoparticles into the liver cannot be avoided, as liver-associated vasculature is also leaky in nature and punctuated with fenestrations (33). However, liver-associated accumulation is not an entirely negative consequence, as this nanoparticle characteristic could be exploited for treatment of liver-associated diseases. In response, we had also shown that micelle-thiostrepton nanoparticles were able to accumulate solely in the liver in normal nude mice, when xenograft tumors were absent (Supplementary data, S4). As it has been described that the suppression of FOXM1 in hepatocellular

carcinomas leads to reduced cancer growth (42), the liver-targeting effect of our nanomedicine system makes it an promising candidate for treatment of liver cancers.

In terms of anti-cancer effects, micelle-encapsulated thiostrepton was further found to reduce the growth rates of MDA-MB-231 breast cancer xenografts and HepG2-luc liver cancer xenografts, compared to that of micelle-only and non-treated controls (Figure 4 and Figure 5). The reduction in tumor growth rate is likely a result of increased cell death in tumor cells, as indicated by the increase in cleaved caspase-3 expression in tumors treated with micelle-thiostrepton (Figure 6). The change in tumor growth rate after thiostrepton treatment is also associated with the suppression of FOXM1 (Figure 6), although at present, exact mechanisms are unknown. FOXM1, as an oncogenic transcription factor, has been shown to be suppressed upon treatment with thiostrepton in human cancer cell lines *in vitro* (1, 2, 5, 43). Here for the first time, we show that thiostrepton inhibits FOXM1 expression *in vivo*, in xenograft tumors, confirming the notion that FOXM1 is general target of proteasome inhibitors (Figure 6). The anticancer effect of micelle-thiostrepton nanoparticles, coupled with their liver-targeting effect, advocates the development of micelle-encapsulated thiostrepton as a novel potential nanomedicine treatment for liver cancer patients.

Supplementary Material

Refer to Web version on PubMed Central for supplementary material.

Acknowledgments

We thank Dr. Angela Tyner (UIC) for the gift of the MDA-MB-231-luc cells, Dr. Susan Uprichard for the HepG2 cells and thanks to Dr. Nissim Hay (UIC) for the gift of the luciferase cDNA in retrovirus vector. Also, we thank Dr. Ke-Bin Low (UIC) for the acquisition of the electron microscope images.

Grant support

This work was supported by NIH grants 1RO1CA1294414 and 1R21CA134615 to ALG.

References

1. Bhat UG, Zipfel PA, Tyler DS, Gartel AL. Novel anticancer compounds induce apoptosis in melanoma cells. Cell Cycle. 2008; 7:1851–5. [PubMed: 18583930]
2. Bhat UG, Halasi M, Gartel AL. Thiazole antibiotics target FoxM1 and induce apoptosis in human cancer cells. PLoS ONE. 2009; 4:e5592. [PubMed: 19440351]
3. Bhat UG, Halasi M, Gartel AL. FoxM1 is a general target for proteasome inhibitors. PLoS One. 2009; 4:e6593. [PubMed: 19672316]
4. Schoof S, Pradel G, Aminake MN, Ellinger B, Baumann S, Potowski M, et al. Antiplasmodial thiostrepton derivatives: proteasome inhibitors with a dual mode of action. Angew Chem Int Ed Engl. 2010; 49:3317–21. [PubMed: 20358566]
5. Pandit B, Bhat UG, Gartel A. Proteasome inhibitory activity of thiazole antibiotics. Cancer Biol Ther. 2011; 11:36–40.
6. Gartel AL. A new target for proteasome inhibitors: FoxM1. Expert Opin Investig Drugs. 2010; 19:235–42.
7. Kalinichenko VV, Major ML, Wang X, Petrovic V, Kuechle J, Yoder HM, et al. Foxm1b transcription factor is essential for development of hepatocellular carcinomas and is negatively regulated by the p19ARF tumor suppressor. Genes Dev. 2004; 18:830–50. [PubMed: 15082532]
8. Pilarsky C, Wenzig M, Specht T, Saeger HD, Grutzmann R. Identification and validation of commonly overexpressed genes in solid tumors by comparison of microarray data. Neoplasia. 2004; 6:744–50. [PubMed: 15720800]

9. Douard R, Moutereau S, Pernet P, Chimingqi M, Allory Y, Manivet P, et al. Sonic Hedgehog-dependent proliferation in a series of patients with colorectal cancer. Surgery. 2006; 139:665–70. [PubMed: 16701100]
10. Dreaden EC, Mwakwari SC, Sodji QH, Oyelere AK, El-Sayed MA. Tamoxifen-poly(ethylene glycol)-thiol gold nanoparticle conjugates: enhanced potency and selective delivery for breast cancer treatment. Bioconjugate chemistry. 2009; 20:2247–53. [PubMed: 19919059]
11. Hawkins MJ, Soon-Shiong P, Desai N. Protein nanoparticles as drug carriers in clinical medicine. Advanced drug delivery reviews. 2008; 60:876–85. [PubMed: 18423779]
12. Perkins WR, Ahmad I, Li X, Hirsh DJ, Masters GR, Fecko CJ, et al. Novel therapeutic nano-particles (lipocores): trapping poorly water soluble compounds. International journal of pharmaceutics. 2000; 200:27–39. [PubMed: 10845683]
13. Adams ML, Lavasanifar A, Kwon GS. Amphiphilic block copolymers for drug delivery. Journal of pharmaceutical sciences. 2003; 92:1343–55. [PubMed: 12820139]
14. Kim TY, Kim DW, Chung JY, Shin SG, Kim SC, Heo DS, et al. Phase I and pharmacokinetic study of Genexol-PM, a cremophor-free, polymeric micelle-formulated paclitaxel, in patients with advanced malignancies. Clinical cancer research : an official journal of the American Association for Cancer Research. 2004; 10:3708–16. [PubMed: 15173077]
15. Roberts WG, Delaat J, Nagane M, Huang S, Cavenee WK, Palade GE. Host microvasculature influence on tumor vascular morphology and endothelial gene expression. The American journal of pathology. 1998; 153:1239–48. [PubMed: 9777955]
16. Maeda H, Wu J, Sawa T, Matsumura Y, Hori K. Tumor vascular permeability and the EPR effect in macromolecular therapeutics: a review. J Control Release. 2000; 65:271–84. [PubMed: 10699287]
17. Ferrari M. Cancer nanotechnology: opportunities and challenges. Nat Rev Cancer. 2005; 5:161–71. [PubMed: 15738981]
18. Gradishar WJ, Tjulandin S, Davidson N, Shaw H, Desai N, Bhar P, et al. Phase III trial of nanoparticle albumin-bound paclitaxel compared with polyethylated castor oil-based paclitaxel in women with breast cancer. J Clin Oncol. 2005; 23:7794–803. [PubMed: 16172456]
19. Lyass O, Uziely B, Ben-Yosef R, Tzemach D, Heshing NI, Lotem M, et al. Correlation of toxicity with pharmacokinetics of pegylated liposomal doxorubicin (Doxil) in metastatic breast carcinoma. Cancer. 2000; 89:1037–47. [PubMed: 10964334]
20. Wu KL, van Wieringen W, Vellenga E, Zweegman S, Lokhorst HM, Sonneveld P. Analysis of the efficacy and toxicity of bortezomib for treatment of relapsed or refractory multiple myeloma in community practice. Haematologica. 2005; 90:996–7. [PubMed: 15996946]
21. Jagannath S, Barlogie B, Berenson J, Siegel D, Irwin D, Richardson PG, et al. A phase 2 study of two doses of bortezomib in relapsed or refractory myeloma. Br J Haematol. 2004; 127:165–72. [PubMed: 15461622]
22. Torchilin VP. Micellar nanocarriers: pharmaceutical perspectives. Pharmaceutical research. 2007; 24:1–16. [PubMed: 17109211]
23. Ashok B, Arleth L, Hjelm RP, Rubinstein I, Onyuksel H. In vitro characterization of PEGylated phospholipid micelles for improved drug solubilization: effects of PEG chain length and PC incorporation. J Pharm Sci. 2004; 93:2476–87. [PubMed: 15349957]
24. Radhakrishnan SK, Bhat UG, Hughes DE, Wang IC, Costa RH, Gartel AL. Identification of a Chemical Inhibitor of the Oncogenic Transcription Factor Forkhead Box M1. Cancer Res. 2006; 66:9731–35. [PubMed: 17018632]
25. Halasi M, Zhao H, Dahari H, Bhat UG, Gonzalez EB, Lyubimov AV, et al. Thiazole antibiotics against breast cancer. Cell Cycle. 2010:9.
26. Maeda H. Tumor-selective delivery of macromolecular drugs via the EPR effect: background and future prospects. Bioconjug Chem. 2010; 21:797–802. [PubMed: 20397686]
27. Lukyanov AN, Gao Z, Mazzola L, Torchilin VP. Polyethylene glycol-diacyllipid micelles demonstrate increased acculumation in subcutaneous tumors in mice. Pharmaceutical research. 2002; 19:1424–9. [PubMed: 12425458]

28. Nasongkla N, Bey E, Ren J, Ai H, Khemtong C, Guthi JS, et al. Multifunctional polymeric micelles as cancer-targeted, MRI-ultrasensitive drug delivery systems. Nano Lett. 2006; 6:2427–30. [PubMed: 17090068]
29. Uster PS, Allen TM, Daniel BE, Mendez CJ, Newman MS, Zhu GZ. Insertion of poly(ethylene glycol) derivatized phospholipid into pre-formed liposomes results in prolonged in vivo circulation time. FEBS letters. 1996; 386:243–6. [PubMed: 8647291]
30. Gabizon A, Papahadjopoulos D. The role of surface charge and hydrophilic groups on liposome clearance in vivo. Biochim Biophys Acta. 1992; 1103:94–100. [PubMed: 1309663]
31. Vonarbourg A, Passirani C, Saulnier P, Simard P, Leroux JC, Benoit JP. Evaluation of pegylated lipid nanocapsules versus complement system activation and macrophage uptake. Journal of biomedical materials research Part A. 2006; 78:620–8. [PubMed: 16779767]
32. Aggarwal P, Hall JB, McLeland CB, Dobrovolskaia MA, McNeil SE. Nanoparticle interaction with plasma proteins as it relates to particle biodistribution, biocompatibility and therapeutic efficacy. Advanced drug delivery reviews. 2009; 61:428–37. [PubMed: 19376175]
33. Braet F, Wisse E. Structural and functional aspects of liver sinusoidal endothelial cell fenestrae: a review. Comp Hepatol. 2002; 1:1. [PubMed: 12437787]
34. Wisse E, Jacobs F, Topal B, Frederik P, De Geest B. The size of endothelial fenestrae in human liver sinusoids: implications for hepatocyte-directed gene transfer. Gene therapy. 2008; 15:1193–9. [PubMed: 18401434]
35. Alexis F, Pridgen E, Molnar LK, Farokhzad OC. Factors affecting the clearance and biodistribution of polymeric nanoparticles. Mol Pharm. 2008; 5:505–15. [PubMed: 18672949]
36. Lukyanov AN, Torchilin VP. Micelles from lipid derivatives of water-soluble polymers as delivery systems for poorly soluble drugs. Adv Drug Deliv Rev. 2004; 56:1273–89. [PubMed: 15109769]
37. Krishnadas A, Rubinstein I, Onyuksel H. Sterically stabilized phospholipid mixed micelles: in vitro evaluation as a novel carrier for water-insoluble drugs. Pharmaceutical research. 2003; 20:297–302. [PubMed: 12636171]
38. Moghimi SM, Hunter AC, Murray JC. Long-circulating and target-specific nanoparticles: theory to practice. Pharmacol Rev. 2001; 53:283–318. [PubMed: 11356986]
39. Greish K. Enhanced permeability and retention of macromolecular drugs in solid tumors: a royal gate for targeted anticancer nanomedicines. J Drug Target. 2007; 15:457–64. [PubMed: 17671892]
40. Matsumura Y, Maeda H. A new concept for macromolecular therapeutics in cancer chemotherapy: mechanism of tumoritropic accumulation of proteins and the antitumor agent smancs. Cancer Res. 1986; 46:6387–92. [PubMed: 2946403]
41. Dvorak HF, Nagy JA, Dvorak JT, Dvorak AM. Identification and characterization of the blood vessels of solid tumors that are leaky to circulating macromolecules. Am J Pathol. 1988; 133:95–109. [PubMed: 2459969]
42. Gusarova GA, Wang IC, Major ML, Kalinichenko VV, Ackerson T, Petrovic V, et al. A cell-penetrating ARF peptide inhibitor of FoxM1 in mouse hepatocellular carcinoma treatment. J Clin Invest. 2007; 117:99–111. [PubMed: 17173139]
43. Kwok JM, Myatt SS, Marson CM, Coombes RC, Constantinidou D, Lam EW. Thiostrepton selectively targets breast cancer cells through inhibition of forkhead box M1 expression. Mol Cancer Ther. 2008; 7:2022–32. [PubMed: 18645012]

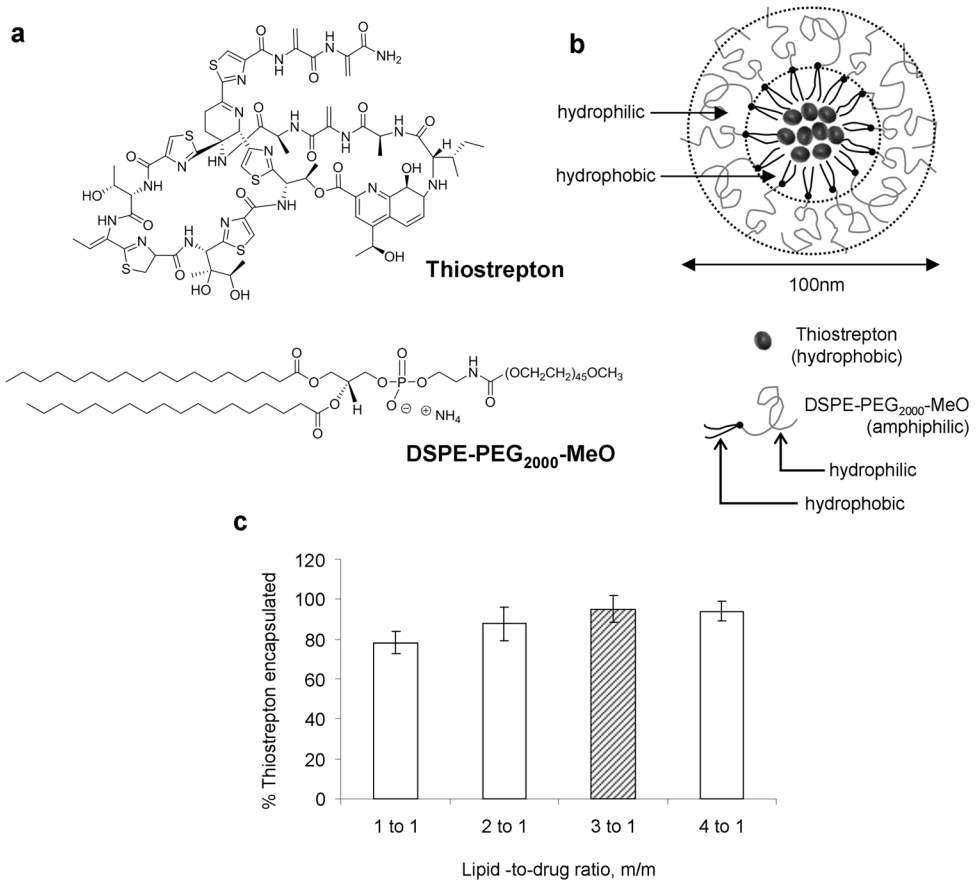

Figure 1.

a) Molecular structures of the thiazole antibiotic, thiostrepton, and DSPE-PEG_{2000}-MeO, the PEGylated amphiphilic lipid used encapsulate thiostrepton into micellar nanoparticles. b) Representation of micelle-thiostrepton nanoparticles, depicting the solubilization of hydrophobic thiostrepton molecules in the inner hydrophobic compartment of the micelle nanoparticle. The nanoparticle is formed by the self assembly of DSPE-PEG_{2000}-MeO and thiostrepton in aqueous solutions. c) Formulation studies to identify the lowest lipid-to-drug ratio required to completely encapsulate 1mM of thiostrepton. 3:1 lipid/drug ratio m/m was identified as the most acceptable ratio for further study. All measurements represent the average of 3 separate experiments, and error bars represent standard deviations.

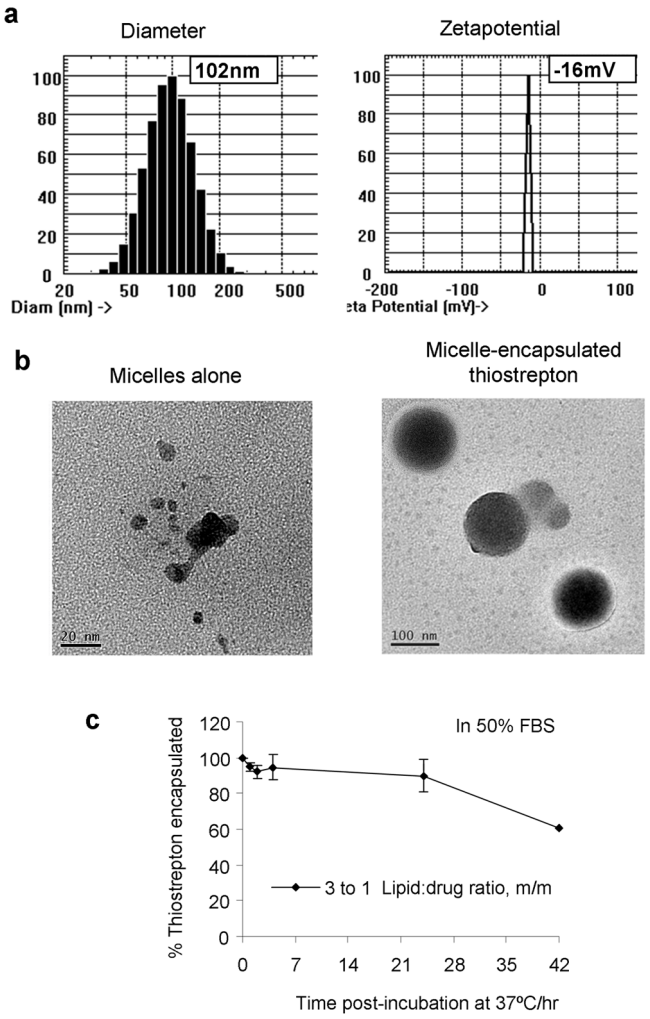

Figure 2.

a) Final nanoparticle-thiostrepton formulations (3:1 DSPE-PEG_{2000}-MeO/thiostrepton, m/m) were found to be approximately 100nm in diameter and −16mV in zetapotential. b) Electron microscopy images of micelles only and micelle-thiostrepton confirm the dimensions of the micelle-encapsulated complexes. c) Release profile of thiostrepton from micellar vehicle (3:1 lipid/drug ratio, m/m) in serum solutions at 37°C that mimic *in vivo* environments (blood circulation). In high serum conditions, thiostrepton can remain encapsulated within micelle nanoparticles for at least 24 hours at 37°C. Each measurement represents the average of 3 separate experiments, and error bars represent standard deviations.

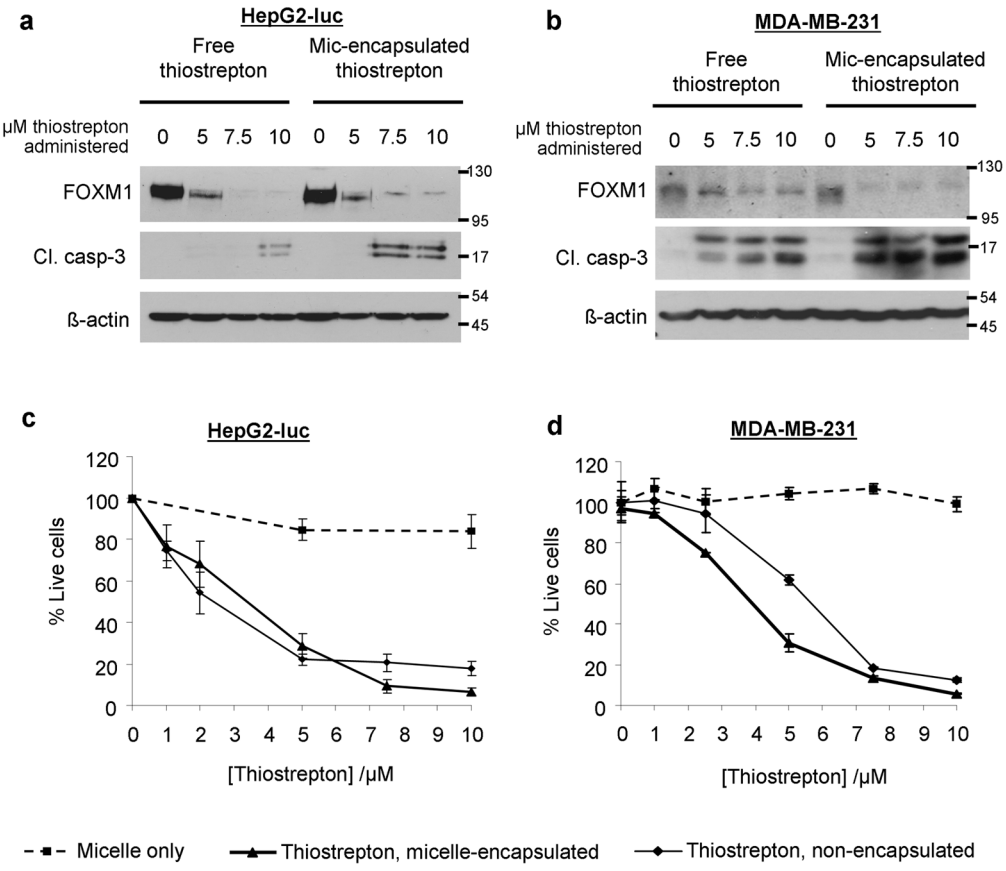

Figure 3.

a) HepG2-luc and b) MDA-MB-231 cells were treated with micelle-encapsulated thiostrepton and non-encapsulated thiostrepton *in vitro*. After 24 hours, cell lysates were examined for expression of the oncogenic transcription factor, FOXM1 and for cleaved caspase-3. The effect of thiostrepton (micelle-encapsulated or non-encapsulated) on cell viability was examined by the MTT assay on c) HepG2-luc cells and d) MDA-MB-231 cells. In all cases, micelle-encapsulated thiostrepton induced greater levels of cell death and inhibited cell viability more efficiently in cancer cells, compared to non-encapsulated thiostrepton. Values represent averages of 4 individual experiments and error bars represent standard deviations.

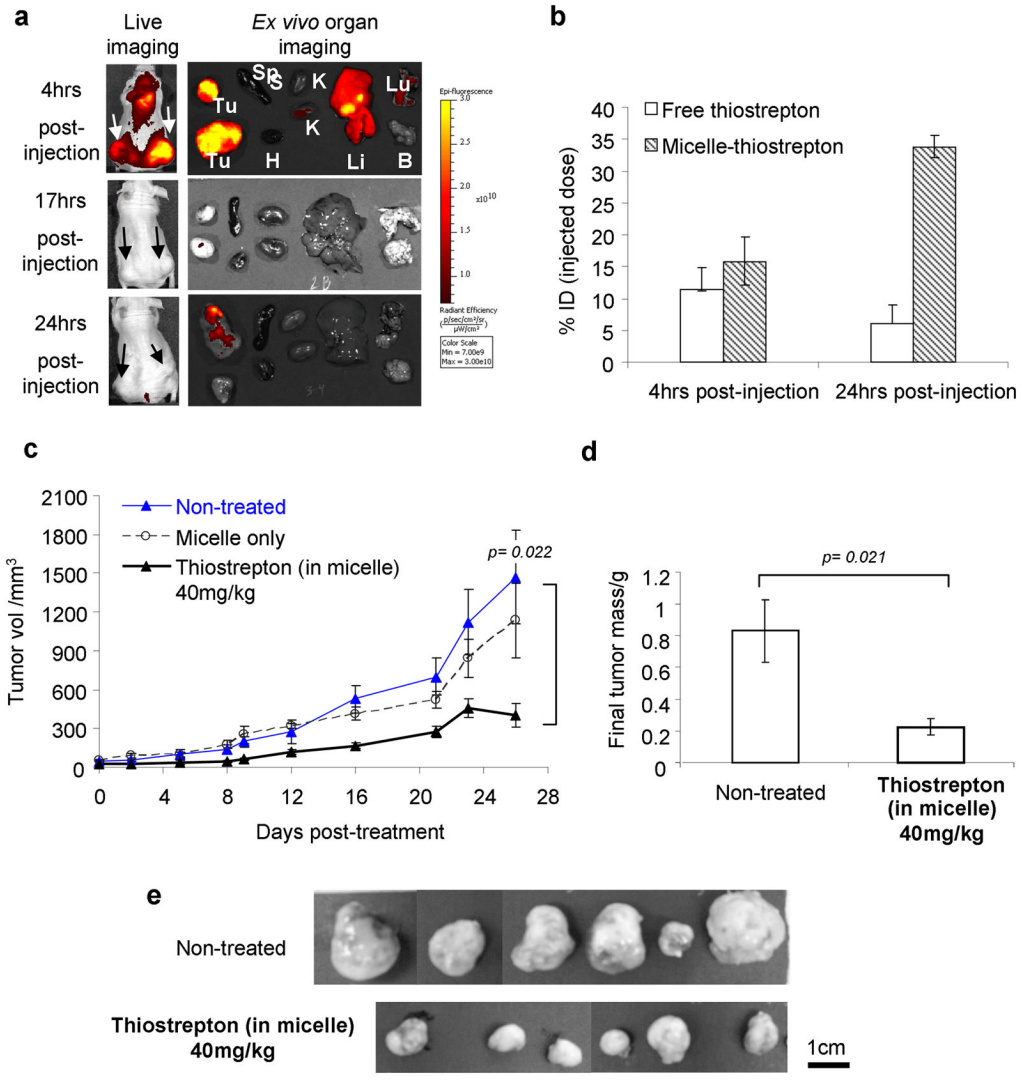

Figure 4.

a) Biodistribution of rhodamine-labeled micelle-thiostrepton complexes in MDA-MB-231 xenograft models. High micelle-associated fluorescence is apparent in tumors (white arrows) and in the liver 4 hours post-injections (Tu=tumors, Sp=spleen, H=heart, K=kidneys, Li=liver, Lu=lungs, B=brain). b) %ID (injected dose) of thiostrepton (either encapsulated in micelles or free) localized in tumors 4 hours and 24 hours after injection. Delivery of thiostrepton through nanoparticle encapsulation increases its accumulation in tumors. Amount of thiostrepton was found by LC/MS on homogenized tumors. *n=2.* c) Anti-cancer effect of micelle-thiostrepton treatment on MDA-MB-231 xenograft volumes, after 14 treatments of 40mg thiostrepton/kg over 26 days, *n= 7–9.* d) Comparison of final MDA-MB-231 tumor weights after completion of treatment schedule, *n=7–9.* Treated tumors were 4-fold lighter in weight than non-treated tumors. e) Final images of harvested non-treated and micelle-thiostrepton-treated tumors. All values represent averages of the quoted *n* numbers. All averages were considered significant, as p values of the Student T test (as quoted in figure) were under 0.03, error bars represent SEM.

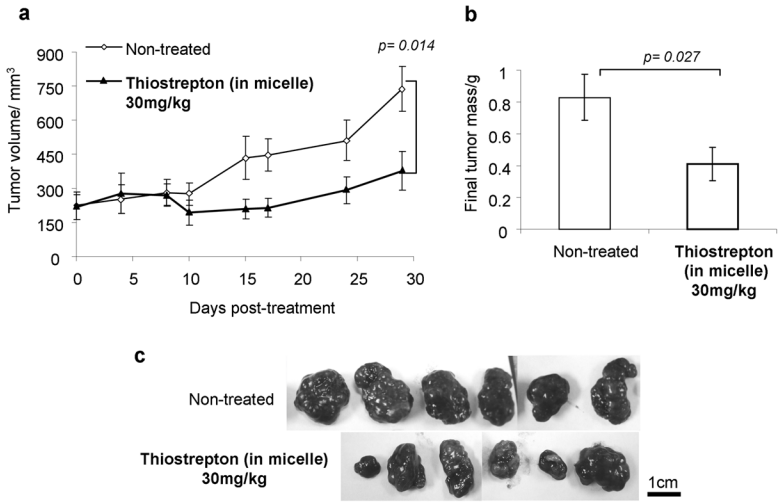

Figure 5.

a) Reduction in HepG2-luc tumor growth, after 11 treatments of 30mg thiostrepton/kg over 28 days, compared to non-treated tumors *n= 6–8*. Error bars represent SEM. b) Comparison of final HepG2-luc tumor weights after completion of treatment schedule, *n=6–8*. Treated tumors were half the weight of non-treated tumors. Error bars represent SEM. c) Photographic images of harvested non-treated and micelle-thiostrepton-treated HepG2-luc tumors. Black bar represents 1cm. All values represent averages of the quoted *n* numbers. All averages were considered significant, as p values of the Student T test (as quoted in figure) were under 0.03, error bars represent SEM.

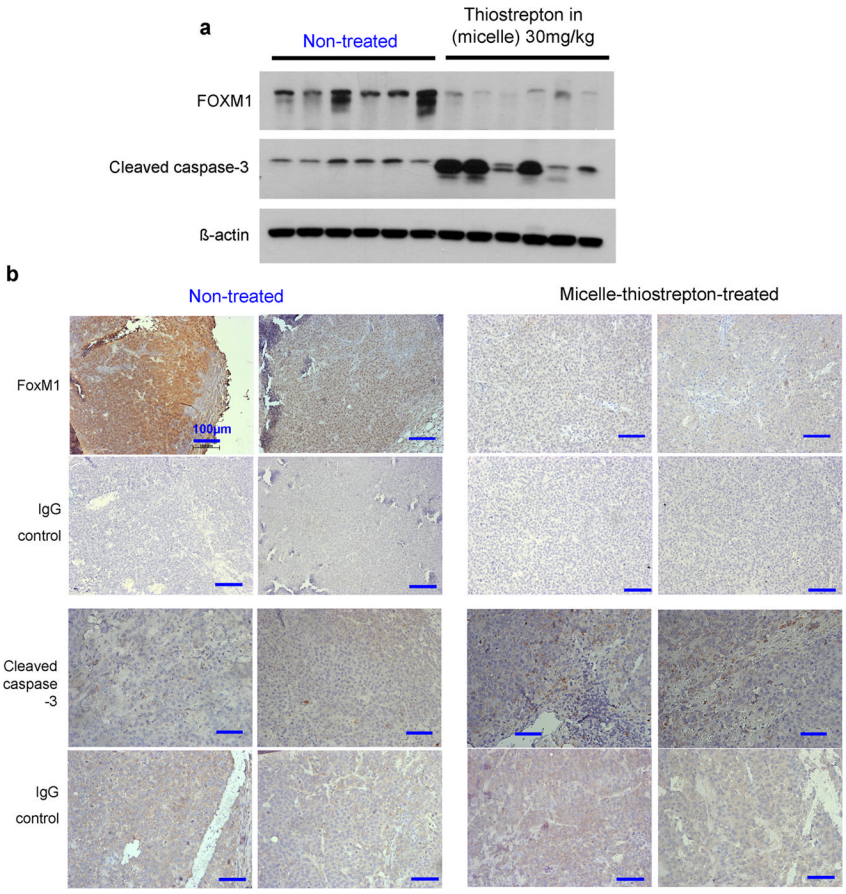

Figure 6.

a) Western blotting of a panel of individual HepG2 tumor homogenates (6 of non-treated and 6 of micelle-thiostrepton-treated) against FOXM1, cleaved caspase-3 and β-actin. FoxM1 expression is evidently suppressed and cleaved caspase-3-associated cell apoptosis is attenuated in tumors treated with micelle-thiostrepton. b) Immunhistochemical analysis of 4 individual HepG2-luc tumors (2 from non-treated and 2 from treated groups) for FOXM1 and cleaved caspase-3 expression (counterstained with hematoxylin). FOXM1 expression is found to be at higher densities in non-treated tumors, compared to thiostrepton-treated tumors. Cleaved-caspase-3 is evidently enhanced in tumors treated with micelle-thiostrepton, identified by the presence of larger numbers of dark, DAB-stained clusters. Control slides were incubated with IgG primary antibodies. Blue bars represent 100μm (20×).